# POWER QUALITY EVOLUTION FOR WIND ENERGY CONVERSION SYSTEMS USING EMBEDDED Z-SOURCE INVERTER AND PERMANENT MAGNET SYNCHRONOUS GENERATOR

RAJENDRAN ELUMALAI<sup>1</sup>, RAJI VARADHAN<sup>2</sup>

Keywords: Permanent magnet synchronous generator (PMSG); Embedded Z-source inverter (EZSI); Total harmonics distortion (THD); Fuzzy logic controller (FLC); Z-source inverter (ZSI); Wind energy conversion system (WECS).

This study focuses on two key goals: maximising wind power and providing the system with high-quality electricity. A permanent-magnet synchronous generator and an embedded Z-source inverter are used in this setup to increase the voltage. The Permanent Magnet Synchronous Generator is employed for its unique features, including excellent performance, low weight and volume, and the fact that it doesn't require an external power source to excite its permanent magnets. The DC-link embedded Z-Source inverter is used to connect this generator to the electrical grid. Typically, the Z-Source connection requires many turns in the transformer winding; however, in this case, lower-rated windings are used for inductance instead of the transformer. Thus, the voltage gain is also balanced by the parallel capacitances. Moreover, symmetrical voltage and current distribution across the network, as well as reduced voltage stresses, are benefits of embedded technology. The recommended method, the embedded Z-Source inverter, is specifically controlled by a fuzzy logic controller that also tracks the maximum power to the wind system and reduces total harmonic distortion by 0.86%, as recorded in MATLAB. However, results were also confirmed from an experimental prototype perspective.

#### 1. INTRODUCTION

A lot of work has been done in recent years to improve power quality using power electronic devices and variable generators. In places where traditional generating is not feasible, small-scale independent wind energy devices are a vital alternative source of electrical energy. Unfortunately, most of these devices cannot capture power at all wind speeds, especially if the wind speed is low, which can be very frequent but low power. Nonetheless, the most effective power conversion from mechanical to electrical energy is provided by contemporary permanent magnets, because it doesn't need an additional DC source for the excitation circuit (winding) and is reliable and safe during normal operation. The permanent magnet synchronous generator (PMSG) has the most benefits of any generator used in wind turbines. Maximising wind energy and supplying the system with high-quality electricity are two of WECS's main objectives. One of the best topologies for WECS to accomplish these objectives is the AC-DC-AC converter. Let's now discuss the literature review articles that follow.

The results of the IG and DFIG systems are displayed and examined in this survey article in relation to the static compensator (STATCOM) in various failure scenarios. The system's drawbacks are enumerated and evaluated. The harmonic content is high, and compensators are required [1]. Although there are many studies on STATCOM-based wind turbine control in fault settings, the main strength of this study is the recommended system's appropriate performance in asymmetrical faults. This section has a high THD and no hardware implementation [2]. A few manageable techniques for lowering the inrush rotor currents are demonstrated based on both linear and nonlinear control strategies. Additionally, the high-voltage ride-through capabilities of DFIG-based WTs is shown. This survey may be used as a guide when selecting a data source and an FRT for a WT system based on DFIG. Grid power is necessary to start electricity generation, and this work does not address harmonics analysis [3]. This paper proposes a WECS system with an ANN controller designed for the supply scheme's reactive power return. The proposed method, DQ theory based on artificial neural

networks, isolates reference current from source current to reduce reactive power and harmonics. Even though the total harmonic distortion (THD) level in this work is 1.1%, a voltage source inverter is used. This inverter cannot function in boost mode when compared to the recommended techniques [4].To assess the effects of several DFIG management modes on power quality in a distribution system for DFIG-supported wind farms, simulated tests have been carried MATLAB/Simulink. The system's response to various operating conditions is simulated and compared. Reactive power guideline and voltage regulation are the two approaches to assess and analyse the simulation outcomes. THD limitations are excluded [5]. An important goal of this smart plan is to talk about the changing plan and hysteresis comparators through a neural regulator to lower the ripple stage of both current and power. The results of the MATLAB simulation show that the neural network provides a decent response, achieves lively operation, and produces reactive power. The fascinating article reveals a high THD level compared to the suggested approach. [6].

The concept and simulation of a PMSG-based wind power generating system under dynamic power system conditions are presented in this study. The active behaviour of the wind control production method is investigated during startup as well as during gust, ramp, and noisy variations of wind conditions using PSCAD/EMTDC simulation [7]. The hardware model and voltage distortion level are not mentioned. This approach makes the system simpler and more robust by doing away with the requirement for a phase-locked loop (PLL). The switching model for controlling the APF is created using an adaptive hysteresis band current controller (AHBCC), which modulates the hysteresis band under scheme constraints while maintaining an essentially constant modulation frequency. To account for reactive power, this study employs a self-tuning filter. As a result, THD was not addressed, and the oldest control method was used [8]. To maximise wind power, a maximum power point tracker (MPPT) is essential, which is why the perturb-and-observe (P&O) strategy is used. Using the MATLAB/Simulink platform, the entire setup is simulated. Time domain results are obtained at different wind speeds and are carefully

<sup>&</sup>lt;sup>1</sup> S.K.P. Engineering College, Tiruvannamalai, Tamil Nadu, India. E-mail: rajendran\_electro@skpec.in

<sup>&</sup>lt;sup>2</sup> S.K.P. Engineering College, Tiruvannamalai, Tamil Nadu, India. Email: raji.vpm@skpec.in

analysed. The author employed straightforward MPPT approaches instead of addressing the THD level [9].

The suggested **MPPT** control method uses straightforward current network to ensure a steady current at the rectifier's output by installing a constant reference in a DC-DC converter connected in series with the rectifier. Power quality was adversely affected by the system's high harmonic content, which resulted from the additional DC-to-DC converter used in this study [10]. There are two types of conventional inverters: current source inverters (CSI) and voltage source inverters (VSI). The following problems impact VSI: The inverter's output voltage cannot be greater than the DC input voltage (buck converter); therefore, the need for an additional voltage boost circuit raises installation costs and often degrades system reliability [11-12]. CSI has further theoretical and conceptual problems, such as being a boost inverter, being costly, having a low line-side power factor, and being susceptible to electromagnetic interference. It is not possible to turn on switches on the same leg of both inverters at the same time. Just to avoid a shot through, which could damage the inverters, this is done [13, 14].

This study has looked at the necessity of including shot through in the control approach. Along with the voltage boost, a connection between the modulation indexes has also been formed. However, the data show that the PMSG's output voltage increases with wind speed, requiring a higher modulation index and a lower boost factor. Furthermore, the findings show that Z-source inverter boost operation can be achieved without additional boost circuitry, thereby reducing costs and simplifying the system [15]. This paper introduces a decoupled current-control method that uses a q-ZSI and dual-frequency modulation (DFM) to regulate both active and reactive power flows in the grid. The MATLAB/Simulink tool is used to comprehensively evaluate the functionality of the proposed controllers through extensive simulations. Finally, their reasonableness is assessed using an experimental hardware arrangement. In this investigation, the grey wolf-optimized MPPT algorithm was employed, which has a longer error settling time than the proposed FLC [16]. The proposed embedded switched-inductor quasi-Z-Source Inverters are simulated and compared with the conventional ZSI and QZSI to assess their high-voltage profiles and performance efficiency. The basic boost pulse-width modulation is then used to simulate PSCAD/EMTDC.

Nevertheless, harmonic profiles are not discussed in this study [17]. The original Z-source inverter (ZSI) connected the DC source to the inverter via an impedance network composed of two inductors and two capacitors arranged in a specific manner. It has buck and boost capabilities that are not available with traditional VSI or CSI. The proposed trans-Z-source inverter has an impedance network consisting of a transformer and one capacitor [18]. We use the modified fractional order PI controller to extract maximum power and ensure a 100% power factor. However, the main issue in this paper is the high total harmonic content and the usage of a basic PI controller [19]. The literature study should conclude by reviewing the different types of wind generators, particularly PMSG, which offers more benefits than IG and DFIG, as discussed in the introduction and abstract chapters. Additionally, boost capabilities are absent from conventional VSI and CSI inverters. As a result, a buck-boost capable embedded

Z-source inverter (EZSI) was presented. The purpose of this article is.

- The goal is to decrease switching stress, along with decreasing the THD.
- The goal is to boost the voltage profile as well as implement the prototype hardware setup model.

# 2. MATERIALS AND METHODOLOGY

A standard AC–DC–AC topology arrangement for PMSG is depicted in Fig.1.

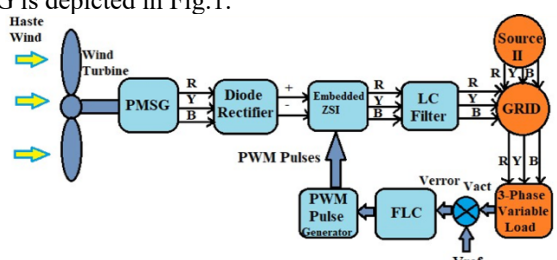


Fig. 1 – Proposed simulation block diagram.

This system comprises a three-phase embedded Z-source inverter and a diode rectifier. According to recent reports, embedded Z-source inverters are a competitive substitute for current inverter topologies and offer a number of builtin benefits, including voltage boost. When switches are turned on during the equivalent inverter phase leg (shootthrough mode), this inverter enables voltage boost capability. Furthermore, because any phase leg of the inverter can experience a short circuit, the system's reliability is significantly increased. Additionally, this setup reduces inverter output power distortion because leg dead time does not need to be phased. This paper's subsection 2.1 presents the embedded Z-Source Inverter and explains how the rectifier that feeds it operates. The fuzzy logic controller and its embedded Z-Source Inverter are accessible in subsection 2.2 of the study.

# 2.1 ANALYSIS OF EMBEDDED Z-SOURCE INVERTER

The voltage-type embedded Z-source inverter, as shown in Fig. 2, differs from a traditional Trans ZSI in that its dc sources are housed in the X-shaped LC impedance network. Its capacitive components C1 and C2 are used to filter voltage, while its inductive elements L1 and L2 are used to filter current. The source current is evened out by the embedded Z-source inverter without need for an extra LC filter. No further filter is needed because the input DC source is divided among the LC impedance. Consequently, no additional strains arise under loading conditions because the DC voltage contribution is separated by Vdc/2. In addition to increasing the output voltage ranges, the embedded Z-source inverter offers voltage ride-through capabilities.

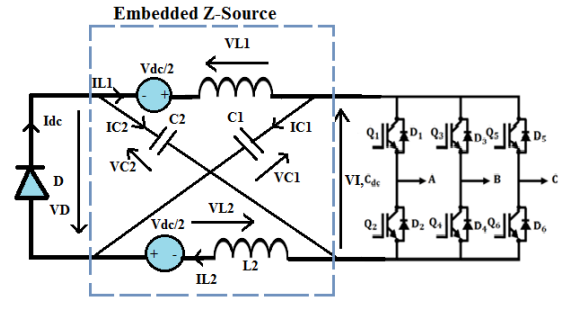


Fig. 2 – Proposed embedded z-source inverter.

# 2.1.1 SHOOT THROUGH MODE

A shoot-through state can be produced, lacking harmful semiconductor devices, by turning on switches beginning the same phase-leg altogether, as shown in Fig. 3. The resulting equivalent circuit illustrates that the inverter bridge is in shoot-through mode and the front-end diode (D) is reverse biased using the blocking-voltage formula as well as previous state equations given below.

$$VD = -2VC, (1)$$

$$VL = VC + \frac{Vdc}{2},$$
 (2)

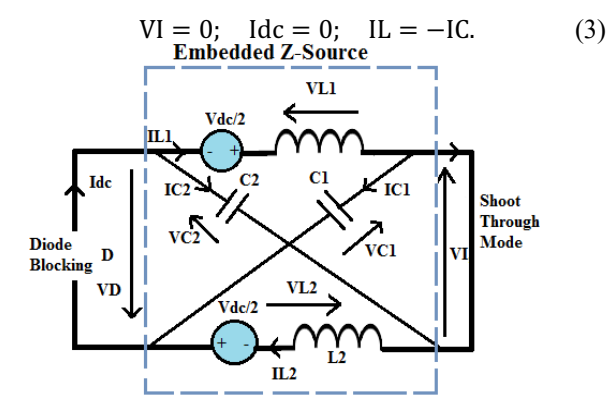


Fig. 3 – Shoot through mode.

#### 2.1.2 NON SHOOT THROUGH MODE

As shown in Fig. 4, while the inverter is in a non-shoot-through state, the diode D conducts, and a current source replaces the output load. In the null state, its value is zero, while in the active state, it is non-zero.

$$VL = \frac{Vdc}{2} - VC * VI = 2VC.$$
 (4)

$$Idc = IL + IC. (5)$$

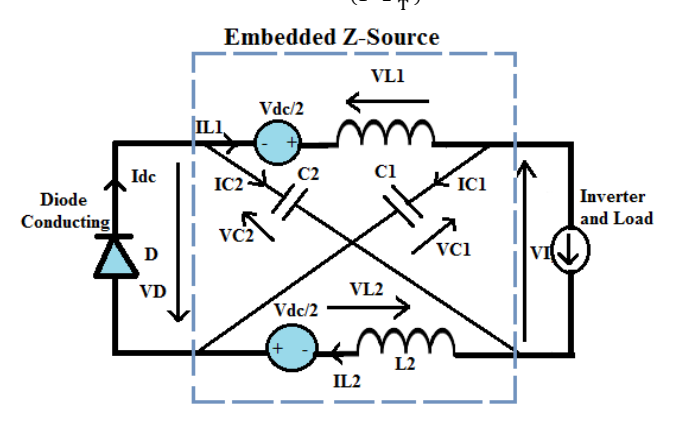
$$Idc \neq 0. \tag{6}$$

which are used to compute the peak dc-link voltage (VP), peak ac output voltage (Vac), and capacitive voltage (VC).

$$VP = \frac{Vdc}{1 - 2\frac{To'}{T}} \tag{7}$$

$$Vac = M * \left(\frac{VP}{2}\right), \tag{8}$$

$$VC = \frac{\left(\frac{Vdc}{2}\right)}{\left(1 - 2\frac{To}{T}\right)},\tag{9}$$



 $Fig.\ 4-Non-shoot-through\ mode.$ 

#### 2. 2 FUZZY LOGIC CONTROLLER

The word "fuzzy" describes how the logic in question can handle ideas that are classified as "partially true" rather than "true" or "false." However, in many situations, alternative methods like neural networks and evolutionary algorithms can outperform fuzzy logic. One benefit of fuzzy logic is that it can solve problems in a way that is easy for human operators to comprehend. Their experience must be incorporated into the controller's design. Because of this, tasks that are currently successfully completed by humans can be mechanized more easily.

The basic architecture of a fuzzy logic controller is shown in Fig. 5. The primary components of an FLC method are an inference engine, a fuzzy rule base, a fuzzy knowledge base, a defuzzifier, and a fuzzifier. Included are normalisation parameters as well. The system is a fuzzy logic decision system when the defuzzifier's output is not a plant control action. The fuzzifier converts fuzzy integers from crisp ones. Details about how the domain capability development operates are contained in the fuzzy rule base. In the fuzzy knowledge base, all of the input-output fuzzy relationship data is stored. The membership functions define the output variables of the plant under control; moreover, the input variables of the fuzzy rule base. The kernel of an FLC method is the inference engine, which may approximate reasoning to reach the required control strategy, simulating human decision-making. The fuzzy quantities are converted into crisp quantities by the defuzzifier from a conditional fuzzy control action near the inference engine.

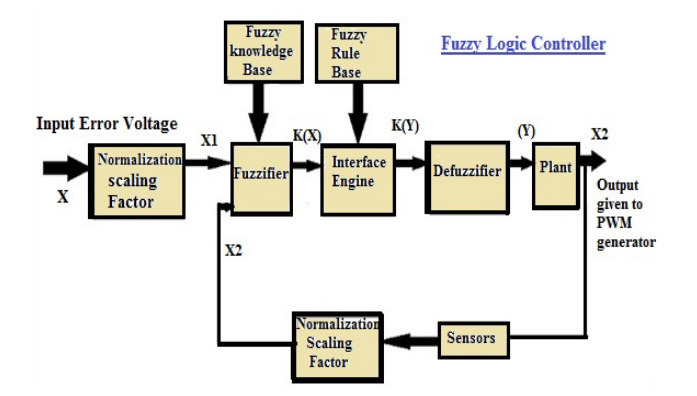


Fig. 5 – Functional diagram of fuzzy logic controller.

#### 3. RESULTS AND DISCUSSION

#### 3.1 SIMULATION RESULTS AND DISCUSSION

As seen in Fig. 6 and Fig. 7, at a wind speed of 1500, the PMSG generates 150V AC, which is then supplied to the diode rectifier.

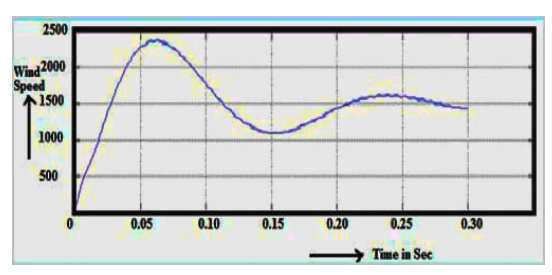


Fig. 6 – Wind speed.

As shown in Fig. 8, the rectifier converts 150 VAC to 150V DC. The EZSI receives this DC supply after that, and depending on the shoot-through ratio, the inverter's DC side can be increased to 550 VDC. 550 VDC is presently converted to 550 VAC via an EZSI, as illustrated in Fig. 9. The FLC inputs were used to run the EZSI, as shown in Fig. 10. The 400V AC is supplied directly to the grid network after the inverter output is filtered. When a second load was introduced, the inverter output current reached 7.5 A after 0.2 s, as illustrated in Fig. 11. At that moment, the inverter current was 1 A. It remained between 0 and 0.2 s when the initial load was applied. If the wind system fails, Source II will supply power to the grid. As seen in Fig. 12, the overall harmonic distortion is 0.86%. The simulation parameters are listed in Table 1.

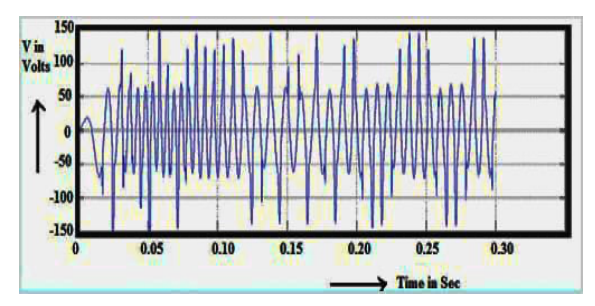


Fig. 7 – PMSG output voltage.

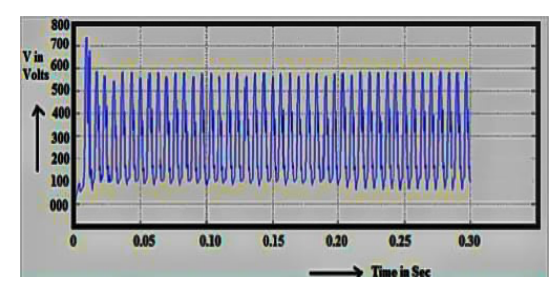


Fig. 8 - Rectifier output voltage.

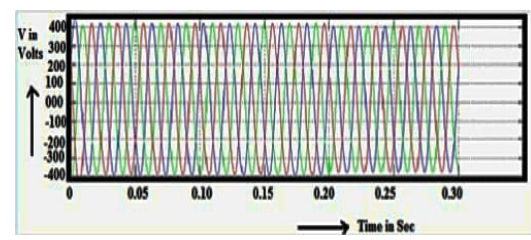
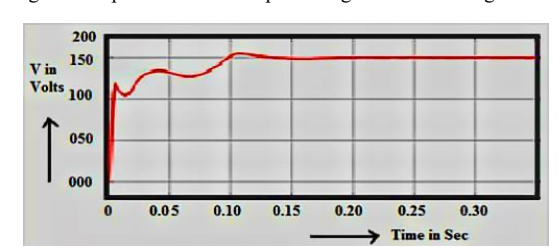


Fig. 9 – Proposed inverter output voltage before filtering circuit.



 $Fig.\ 10-Proposed\ inverter\ output\ voltage\ after\ filtering\ circuit.$ 

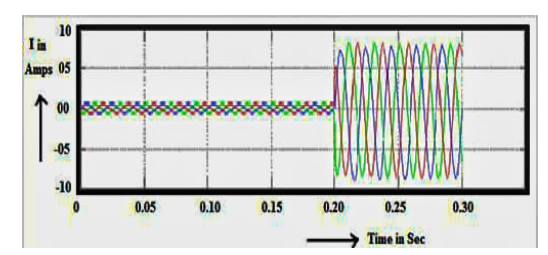


Fig. 11 – Proposed inverter output current after filtering circuit.

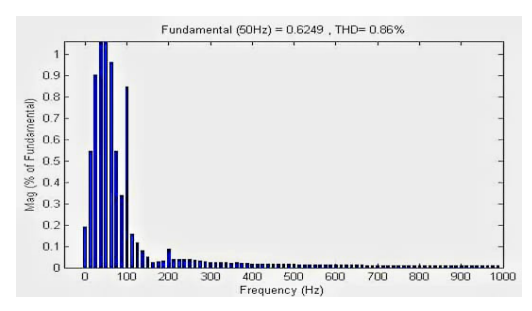


Fig. 12 – THD for the after filtering circuit.

#### 3.2 EXPERIMENTAL RESULTS AND DISCUSSION

A hardware block diagram and a picture of a prototype are shown in Figs. 13 and 14, respectively.

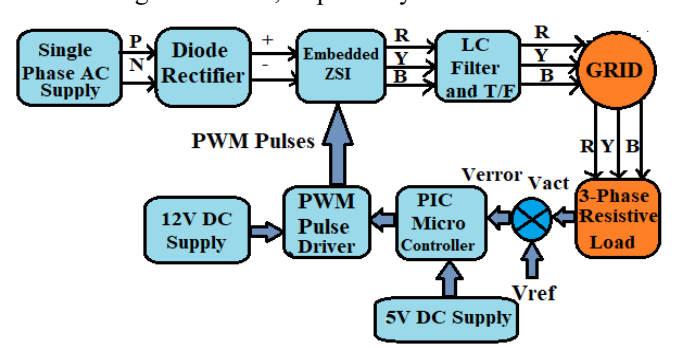


Fig. 13 – Hardware block diagram for proposed system.

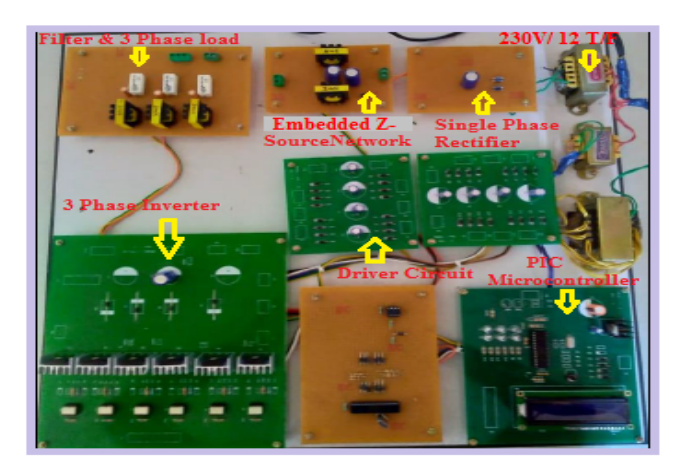


Fig. 14 – Snapshot for proposed EZSI system.

The proposed method used a 12 V AC supply to power an unregulated (diode) rectifier circuit. With this single-phase unregulated rectifier, a 12 V AC supply is converted to a 12 V DC supply. It is delivered to the EZSI at 12 V DC. The shoot-through state is utilized in the implementation of this EZSI. The shoot-through mode is used to increase the DC side 12 V DC supply to a 48 V DC supply. By converting the Embedded ZSI's 48 V DC output to 48 V AC, the threephase inverter also reveals the DSO output voltage Fig.15. To filter the output voltages from inverters, LC filters are employed. After that, the transformer receives an LC-filtered output voltage at the same frequency as the grid. The transformer output voltage is ultimately connected to the grid system. Given that this load is entirely resistive, any changes in load could cause the signal to conditionally detect changes in voltage. Depending on changes, FLC gives the comments to produce the inverter's firing pulse. The THD and Frequency waveform of the proposed embedded Z-source network-enabled 3-phase voltage source inverter is shown in

Fig. 16. Since the proposed system only deviates the voltage THD (1.887%) and output current THD (2.481%), along with the frequency 49.831 Hz obtained from the frequency and harmonics analyzer hardware tools, it conforms to the IEEE harmonics standard.

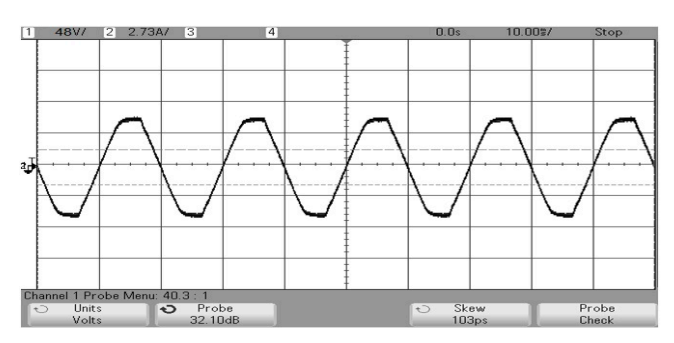


Fig. 15 - Embedded Z-source inverter output voltage (48 V) from DSO.

rmai Mode		Peak Uver Scaling = L		ine Filter Time		iteg: Keset	YOKOGAWA	
				reg Filte			PLL1: 49.831	
		Order	U2 [V] hdf[%]	Order		hdf[%]	0F:3	
		Total	0.00	Total	0.0003	IKIT [AI]	Element 1 ::	
fPLL1:15	49.831 Hz	dc	-0.00 -72.642	dc	-0.0003	0 F	01 150V 11 2A	
fPLL2:14	49.842 Hz	1	0.00 100.000	1	0.0000	100,000	Sync Src: 11	
		2	0.00 6.864	2	0.0000	52.342	Element 2 K	
Irms4	71.863 V	3	0.00 62.179	3	0.0000	80.741	U2 100V 12 2A	
Irms4	1.2748 A	4	0.00 10.259	4	0.0000	54.360	Sync Src: 12	
P4	90.89 #	5	0.00 42.526	5	0.0000	23.340	Element 3	
S4	91.61 VA	6	0.00 5.812	6	0.0000	89.425	U3 100V	
Q4	11.47 var	7	0.00 27.113	7	0.0000	58.194	13 2A Sync Src: E	
λ4	0.9921	8	0.00 32.111	8	0.0000	39.954	Element 4	
Φ4	67.19 °	9	0.00 47.153	9	0.0000	47.898	U4 60V	
		10	0.00 7.232	10	0.0000	42.935	14 2A	
Uthd4	1.887 %	11	0.00 12.438	- 11	0.0000	16.627	Sync Src: E	
Ithd4	2.481 %	12	0.00 13.573	12	0.0000	18.190	Element 5	
Pthd4	0.025 %	13	0.00 11.669	13	0.0000	9.923	U5 60V 15 2A	
Uthf4	0.792 %	14	0.00 38.732	14	0.0000	18.856	Sync Src: E	
Ithf4	1.887 %	15	0.00 41.455	15	0.0000	30.693	Element 6	
001111	0 F	16	0.00 27.604	16	0.0000	43.789	U6 60V	
	0 F	17	0.00 22.426	17	0.0000	44.694	6 2A Symc Src: [13]	
hvf4	1.090 %	18	0.00 6.984	18	0.0000	14.928		
hcf4	2.481 %	19	0.00 54.864	19	0.0000	42.042		
Kfact4	1.1833	20	0.00 10.339	20	0.0000	65.934		
PAGE 4/	□PAGE□ 4/11 □PAGE□ 1/25							

Fig. 16 – EZSI output voltage THD (1.887%), output current THD (2.481%), and output frequency (49.831 Hz).

# 4. CONCLUSION

This study's well-known embedded Z-Source Inverter has simplified the process of connecting the output power to the grid network. A novel framework for fuzzy logic control is presented in this study. The THD level of the proposed model was 0.86% (Fig. 12) compared to the excited model [4]. MATLAB Simulink generates exciting models with THD values higher than 3.0%. Furthermore, the voltage boosting ratio is low for typical VSI, CSI, and basic Z-Source inverters. The state performance and output evaluation of the suggested simulation are demonstrated to be fairly reasonable. The prototype hardware arrangement successfully reaches the suggested enhanced voltage profile EZSI output voltage 48 V (Fig.15), while keeping the IEEE Standard reduced THD value and rated frequency (Fig.16).

This study examines the usefulness of experimental prototype hardware models and MATLAB simulations, and its goal is accomplished. Future windmill installations around the world could be a significant source of wind control innovation, since they require less equipment than conventional wind turbines and can connect to wind power produced in low-wind areas.

### CREDIT AUTHORSHIP CONTRIBUTION

Author\_1: Contributed equally to the current study at every level, from problem formulation to results and resolution.

Author\_2: Contributed equally to the current study at every level, from problem formulation to results and resolution.

#### **APPENDIX**

Table 1
Simulation parameters

Specifications	Rating				
Grid	400 V, 50 Hz				
PMSG Stator Phase	1.6 Ω, 11.3 mH				
resistance, inductance					
LC Filter	1000 Ω, 10 mH				
RLC branch	$0.0001 \Omega, 2e^{-3} H$				
3-phase Source	400 V, 50 Hz				
3-RLC Load	$400 \text{ V}, 50 \text{ Hz}, P = 5.5e^3 \text{ QL} = 500, \text{ QC} = 500$				
	50 Hz, 400 V, Lm=500 pu,				
Transformer	$Rm = 500 \text{ pu}, L_1 = 0.08 \text{ pu}, L_2 = 0.08 \text{ pu}, R_1 =$				
	$0.002 \text{ pu}, R_2 = 0.002 \text{ pu},$				

# **ACKNOWLEDGEMENTS**

I wish to express my gratitude to my beloved Principal, Dr. S. Baskaran, for providing us with the opportunity to do the research work. I want to express my heartfelt thanks to My Parents, Mr. P. Elumalai and Mrs. E. Rukkumani. My beloved wife, Dr. I. Vijaya Lakshmi, B.S.M.S., and My Sweetheart Sons, Mr. R. Renu Prasaath and Mr. R. Sriram, for supporting me regularly. Finally, I express my sincere gratitude to my co-author, Dr. V. Raji, and the SKPEC management for their ongoing support.

Received on 23 January 2025

#### REFERENCES

- M.E. Şahin, Comparison of IG and DFIG for wind power generation systems, Gazi Journal of Engineering Sciences, 6, 3, pp. 230–241 (2020).
- N.G. Khani, Improving fault ride-through capability of induction generator-based wind farm using static compensator during asymmetrical faults, Electrical Energy System (2021).
- A.P. G and H.S. H, A comprehensive review of fault ride-through capability of wind turbines with grid-connected doubly fed induction generator, Int Trans Electr Energy Syst (2020).
- R. Elumalai, Maximum power quality tracking of ANN controllerbased DFIG for wind energy conversion system, Rev. Roum. Sci. Techn. – Électrotechn. et Énerg., 69, 2, pp. 189–192 (2024).
- G. Shahgholian and S.M. Zanjani, A study of voltage sag in distribution system and evaluation of the effect of wind farm equipped with doubly-fed induction generator, Rev. Roum. Sci. Techn. – Électrotechn. et Énerg., 68, 3, pp. 271–276 (2023).
- I. Yaichi and A. Semmah, Control of doubly-fed induction generator using artificial neural network controller, Rev. Roum. Sci. Techn. – Électrotechn. et Énerg., 68, 1, pp. 46–51 (2023).
- M. Mohan and K.P. Vittal, Modeling and simulation of PMSG-based wind power generation system, In IEEE Xplore, 3rd IEEE International Conference on Recent Trends in Electronics, Information & Communication Technology (RTEICT) (2018).
- P. Chaturvedi and D.K. Palwalia, PMSG-based standalone wind energy conversion system with power quality enhancement, International Journal of Renewable Energy Research-IJRER, 13, 2 (2023).
- S. Data, A. Islam, T. Saikia, and S. Adhikari, Performance study of a grid-connected permanent magnet synchronous generator-based wind turbine system, In IEEE Xplore, International Conference on Computer, Communication, Chemical, Materials and Electronic Engineering (IC4ME2) (2020).
- A.J. Balbino, B.D.S. Nora, and T.B. Lazzarin, An improved mechanical sensor less maximum power point tracking method for permanent-magnet synchronous generator-based small wind turbine systems, IEEE Trans Ind Electr, 69, 5, pp. 4765–4775 (2021).
- S. Piriienko, T. Röser, M. Neuburger, and A. Balakhontsev, Current source gate drivers for 3-phase VSI operated in small-scale wind

- turbine systems, International Journal of Electrical Power & Energy Systems, 141 (2022).
- 12. A.Chakrabarti, P.K. Sadhu, and P. Pal, A novel dead-time elimination strategy for voltage source inverters in induction heating systems through fractional order controllers, Rev. Roum. Sci. Techn. Électrotechn. et Énerg., 67, 2, pp. 181–185 (2022).
- Z. Alnasir and M. Kazerani, Dynamic average modeling of a CSIbased small-scale standalone wind energy conversion system, In IEEE Xplore, 2018 IEEE Electrical Power and Energy Conference (EPEC) (2019).
- 14. X. Tan and J. Dai, A novel converter configuration for wind applications using PWM-CSI with diode rectifier and buck converter, Electrical Engineering (2011).
- S.A. Kamilu, A. Mohammed, B. Ummai, S. Ikuforiji, A. Michael, and A. Muyideen, Maximum boost PWM control technique of threephase ZSI-based wind energy conversion systems, International Journal of Scientific Research in Science, Engineering and Technology, 6, 5, pp. 191–201 (2019).

- S. Nath, H.C. Nannam, and A. Banerjee, Grey wolf-optimized MPPT controller for q-ZSI-based grid-tied wind power generation system, Electr Eng, 106, pp. 3445–3460 (2024).
- M. Abbasi, A.H. Eslahchi, and M. Mardaneh, Two symmetric extended-boost embedded switched-inductor quasi-Z-source inverter with reduced ripple continuous input current, IEEE Transactions on Industrial Electronics, 65, 6, pp. 5096–5104 (2018).
- O.B. Heddurshetti, J. Chavan, S. Sanadi, V. Patil, and K. Magadum, Design and implementation of trans-Z-source inverter, International Journal of Emerging Technologies and Innovative Research, 5, 9, pp. 762–766 (2018).
- A. Beddar, H. Bouzekri, B. Babes, and H. Afghoul, Real-time implementation of improved fractional order proportionalintegral controller for grid-connected wind energy conversion system, Rev. Roum. Sci. Techn. – Électrotechn. et Énerg., 61, 4, pp. 402–407 (2016).